RSC Advances

ROYAL SOCIETY OF CHEMISTRY

www.rsc.org/advances

A novel label free aptasensor based on target-induced structure switching of aptamers functionalization mesoporous silica nanoparticle

Lili Du[1], Yu Zhang[1], Yan Du, Dongzhi Yang, Fenglei Gao*, and Daoquan Tang*

Jiangsu Key Laboratory of New Drug Research and Clinical Pharmacy, School of Pharmacy, Xuzhou Medical College, 221004, Xuzhou, China.

Abstract: In this paper, a sensitive protocol for high-performance liquid chromatography (HPLC) detection of adenosine triphosphate (ATP) is designed based on mesoporous silica nanoparticles (MSN) functionalized with an aptamer as cap has been designed. The aminopyrine (AP) was sealed in the inner pores of MSN with single-stranded DNA. In the presence of ATP, the ATP aptamer combined with ATP and got away from the pore, and thus opens the DNA biogate to release the AP. The released signal tags can be easily read out by HPLC. The designed protocol provides a sensitive HPLC detection of ATP down to 0.41 nM with a linear range of 4 orders of magnitude (from 1.0 nM to 10 μM) and has high selectivity toward its target ATP, which can be attributed to the large loading capacity and highly ordered pore structure of mesoporous silica nanoparticles, as well as the selective binding of aptamer with ATP. This proof of concept might promote the application of ATP-responsive devices and can also provide an idea to design various target-responsive systems using other aptamers as cap.

Keywords: chromatography, mesoporous, aptamer, ATP,

---

*Corresponding author. Tel./Fax: +86-516-83262138.

Email address: jsxzgfl@sina.com (F. Gao); tdq993@hotmail.com (D. Tang).

1. These authors contributed equally to this work.

Introduction

Adenosine triphosphate (ATP), a major cellular energy currency, plays an important role in the regulation of cellular metabolism and supplies energy for various biochemical reactions in almost every organism[1,2]. ATP involves the regulation of DNA replication, biosynthesis, membrane ion-channel pump, hormonal and neuronal activities and effects in every organism[3-5]. Abnormal concentration of ATP has been reported to be tightly associated with cardiovascular, Parkinson's and Alzheimer's diseases, and it also has been widely used as an indicator in disease diagnoses such as cell viability and injury[6,7]. In addition, ATP is often used as an indicator of microbial contamination, in which the content of ATP reflects the degree of contamination. Therefore, the accurate detection and quantification of ATP is important for biochemical, clinical, and food hygienical applications[8-10].

ATP is usually detected using chromatographic[11,12], mass spectrometry[13], chemiluminometric, and bioluminometric methods[14,15]. Mass spectrometry is accurate but equipment-expensive, both bioluminescence and chemiluminescence method involve chemical reactions among multiple components, especially the enzymes used in bioluminescence are costly and unstable. High-performance liquid chromatography (HPLC) is one of the most suitable techniques for simultaneous analysis of different compounds at analytical (or preparative) levels because of its high efficiency, speed, reproducibility, and wide range of applications[16, 17]. However, most of these reported methods lack the process of signal amplification, so their sensitivities are relatively lower than those of the biosensors. In addition, the use of antibodies as affinity

stationary phases has constraints such as low surface loading, batch-to-batch reproducibility, low surface loading capability can be amended by suitable construction of conjugated antibodies.

In recent years, the aptamer-based ATP sensing strategy has attracted a tremendous interest because of the specific binding between selected aptamer and ATP[18,19]. Aptamers are single-stranded nucleic acids isolated from randomsequence DNA/RNA libraries by an in vitro selection process termed the systematic evolution of ligands by exponential enrichment (SELEX)[20,21]. Compared with antibodies or enzymes, aptamers would be promising molecular probes for bioanalytical applications because of their simple synthesis, easy labeling, good stability, high affinity and specificity with various kinds of targets[22,23]. Aptamers have specially witnessed a substantial progress in bioanalytical fields[24-26]. Many different methods of chemical modification for aptamers have been developed to functionalize them with various functional groups. Since, aptamers can be adopted for any target molecule and because of their endless opportunities for chemical modifications, they could be considered as very attractive detection and diagnostic tools in various bioassays[27,28]. Up to now, many different aptamer-based sensors (aptasensors) for various kinds of targets including small molecules, pharmaceutical drugs, biological macromolecules, and even whole cells have been successfully fabricated[29,30]. To the best of our knowledge, there is no report focusing on target-responsive controlled cargo release from mesoporous silica for the development of high-performance liquid chromatography until now.

Mesoporous silica nanoparticles (MSN) contain hundreds of channels (mesopores)

arranged in a 3D network of honeycomb-like porous structure[31-33]. Due to the highly ordered pore structure, biocompatibility large loading capacity, and adjustable pore size, ease of functionalization, MSNs have attracted substantial research attention in the fields of biotechnology and nanomedicine[34-36]. Particularly, some signal molecules can be filled in the mesopores of MSN and then sealed with different gatekeepers such as nanoparticles, organic molecules, supramolecules, and biomolecules to construct stimuli responsive MS nanoprobes. Various stimuli, such as heat, magnetic fields, pH, target molecules, enzymes, or even light, have been implemented to trigger the opening of the pores and controllable release of the encapsulated substrates[37- 43]. These stimuli-responsive MSNs are frequently used as delivery vehicles and sensory nanoprobes. For example, a fluorescent dye has been entrapped within a MSN for fluorescence assay ATP, but they all need to require the labeling of the probes for attachment on the Au nanoparticles or MSN surfaces, which basically increase the complexity and cost for ATP monitoring[27,28]. In this paper, we report a novel label-free ATP aptasensor based on target-induced structure switching of aptamers functionalization MSN.

This work made use of the flexible binding properties of the negatively charged DNA for electrostatic adsorption the positively charged aminefunctionalized MSNs to seal aminopyrine (AP) in the mesopores, which excluded the steric hindrance of the complex formed on MSN to AP release and simplified the sealing procedure of AP. The aptamer DNA strand could conveniently detach from the MSN surface upon its hybridization with target ATP. The assay is carried out based on target-responsive

controlled release of AP from aptamer-gated mesoporous silica nanocontainer. Initially, AP is loaded into the pores of mesoporous silica, and the pores are then capped with aptamer. Upon target introduction, the molecular gate is opened, resulting in the cargo release from the pores. The released AP can be quantitatively monitored by a HPLC. By monitoring the shift in the HPLC intensity, we could quantitatively determine the content of target ATP in the sample.

2. Experimental

2.1 Reagents and Materials.

Adenosine 5′-triphosphate (ATP), guanosine 5′-triphosphate (GTP), cytosine 5′-triphosphate (CTP), and uridine 5′-triphosphate (UTP), tetraethylorthosilicate (TEOS, 28%) and 3-aminopropyltriethoxysilane (APTES) were purchased from Sigma-Aldrich (USA). Milli-Q water (resistance >18 MΩ cm) was used in all experiments.

Hybridization buffer (HB, pH 7.4) contained 10 mM Tris-HCl, 50 mM NaCl, and 10 mM $MgCl_2$. The washing buffer was PBS (0.1 M, pH 7.4) containing 0.05% (w/v) Tween-20. ATP aptamer was obtained from Takara (Dalian, China), the oligonucleotide was as follows: ATP-aptamer: 5’-CACCTGGGGGAGTATTGCGGAGGAAGGTT-3′ [28].

2.2 Apparatus.

The HPLC analysis was performed on System Shimadzu LC-20AD. Separation was performed on a Diamonsil C18 column (200×4.6mm，5μm). The mobile phases used for elution were H_2O:CH_3OH = 35:65 (v/v). The injection volume was 20 μL,

flow-rate was 1 mL/min and detection was obtained at a wavelength of 259 nm. The transmission electron microscopic (TEM) images were obtained on a JEM-2100 transmission electron microscope (JEOL Ltd., Japan). Nitrogen absorption/desorption measurement was obtained with a porosimeter (ASAP 2020, Micromeritics, USA). Dynamic light scattering (DLS) was observed on 90 Plus/BI-MAS equipment (Brookhaven, USA). Zeta-potential analysis was performed on a Zetasizer (Nano-Z, Malvern, UK).

2.3 Preparation of MSN.

The MSNs were first synthesized with the following procedure[47]. First, 1.75 mL of NaOH (2.00 M) was added to 240 mL of CTABr (2 mg mL^{-1}) and heated to 95 °C. Under continuous stirring, 2.5 mL of TEOS was added dropwise. The mixture was allowed stirring for 3 h to give a white precipitate. Then the solid product was centrifuged, washed with deionized water and ethanol, and dried at 60 °C overnight. The obtained white powder was finally calcined at 550 °C using oxidant atmosphere for 5 h to remove the template phase. Next, 0.5 g of calcined MSNs and 0.5 mL of APTES were suspensed in 50 mL of anhydrous ethanol inside a round-bottom flask. After the mixture was stirred continuously for 6 h at 36 °C, it was filtered, washed with ethanol, and dried at 60 °C to obtain amine-functionalized MSNs.

2.4 AP Loading and Capping.

Then, 1 mg of amine-functionalized nanoparticles was dispersed in 1 mL of HB containing 35 mg mL^{-1} AP. The mixture was shaken overnight in the dark at room temperature and then was centrifuged and washed with ultrapure water to obtain

AP-loaded MSNs, which were further suspended in 1 mL of HB containing 0.04 mM DNA (aptamer) and shaken for 60 min at room temperature. The resulting solids were isolated by centrifugation and washed with hybridization buffer to obtain MSNs.

2.5 AP Releasing.

The detection was performed by mixing 100 μg of MSN with 10 μL of various concentrations of ATP and the reaction solution was mixed with 100 μL HB for incubation at 37 °C for 60 min. Subsequently, 0.1 mL of supernatant was taken periodically from the suspension at 25 °C followed by centrifugation (15 000 rpm, 10 min). The release of AP from the pore voids to the buffer solution was determined by HPLC.

3. Results and discussion

3.1. Principle of the proposed method.

The working principle of the aptamer-target interaction responsive controlled-release system is illustrated in Scheme 1. In this work, MSN could be utilized as the building block for the encapsulation of AP. The solid MSN were first functionalized with APTES to present aminopropyl groups on the wall of mesopores. The functionalized MSN were then loaded with AP. After APTES modification, the MSN became positively charged, the positively charged MSN was demonstrated to be beneficial for electrostatic adsorption of the negatively charged aptamer. Because the flexibility of the single stranded DNA displayed good coverage of the MSN pores, the MSNs remained “capped” at this stage. In the absence of ATP, the pores of MSN were blocked, and the leakage of guest molecules was inhibited. In the presence of ATP, a

competitive reaction took place due to higher affinity and tighter binding of ATP aptamer with ATP, resulting in the opening of pores and the release of guest molecules. The released AP can give rise to the enhanced of HPLC signal. Consequently, the HPLC signal increased directly depends on the concentration of target in the sample, resulting in improved sensitivity for low-abundance ATP detection.

3.2. Characterization of MSN.

The morphology of MSN was characterized by TEM (Fig. 1A), which showed a porous structure of the uniform MSN with a diameter around 120 nm. The size of MSN was verified by DLS measurement (Fig. 1B). In addition, the DLS results also reflected the good dispersity of MSNs in aqueous medium, which was essential for biological application. The nitrogen adsorption−desorption isotherm of the MSNs showed an average pore diameter of 2.5 nm (Fig. 1C), which was in agreement with the porosity reflected by the TEM image. The total pore volume and total specific surface of MSNs were calculated to be 0.76 $cm^3\ g^{-1}$ and 860.5 $m^2\ g^{-1}$ by using the BJH and BET model on the adsorption branch of the isotherm, respectively. Zeta-potential analysis was used to characterize the preparation of MSN (Fig. 1D). After functionalization with APTES, the MSNs became positively charged indicating that the amine groups were successfully functionalized on the surface of MSNs (column b). The entrapment of AP slightly increased the positive charge of the MSN (column c). The positively charged amine functionalized MSNs were beneficial for electrostatic adsorption of the negatively charged DNA, resulting in a negatively charged MSN (column d). This result indicated the successful attachment of DNA on the surface of

MSN. The amount of DNA attached on MSN was determined to be 0.0364 mmol per gram of MSNs[44].

3.3 Feasibility of the proposed method.

To prove the design, the feasibility of the developed strategy was confirmed by HPLC detection. As shown in Fig. 2, in the absence of target ATP, the signal intensity of HPLC at 2.5 min (curve b) was the same as the blank (curve a), which result from HB solvent. The signal intensity of HPLC at 6 min was substantially lower, and these may be attributed to desorption of residual AP from surface domains at the exterior of the pores, or to the slow leakage of AP from the incompletely blocked pores. In the presence of 10 μM of ATP, the incubation of MSN with the ATP led to much stronger HPLC signal intensity (Fig. 2, curve c), which reflected the recognition of the target ATP by aptamer to form complex and lead to the dissociation of aptamer from the MSN surface by the hybridization of complex with ATP, which resulting in the opening of the pores. Moreover, the peak increased with the time (curve d), indicating that more AP was released from the aptamer−MSN system. To verify that the evidence of the adsorption of ATP-aptamer complex into the solid phase of HPLC, hybridization tests using water as solvent were performed. As shown in Fig. S1, in the absence of target ATP, the signal intensity of HPLC at 2.5 min (curve b) was no peak and the same as the blank (curve a). The signal intensity of HPLC at 6 min was substantially lower (curve b), and these be attributed to the slow leakage of AP from the incompletely blocked pores. In the presence of 10 μM of ATP, the incubation of MSN with the ATP led to much stronger HPLC signal intensity at 6 min (Fig. S1, curve c), and a new peak

has appeared at 2.5 min that be attributed to the adsorption of ATP-aptamer complex into the solid phase of HPLC, which reflected the recognition of the target ATP by aptamer to form complex and lead to the dissociation of aptamer from the MSN surface. This result showed that ATP could easily destroy the adsorption between aptamer and MSN system and form a very stable aptamer-ATP structure at room temperature, indicating that ATP is a good stimulus to uncap the MSN pore and release the trapped AP molecules.

3.4 Optimization of detection conditions.

As the HPLC signal resulted from the released AP, the amount of AP in the mesopores, which depended on its concentration used for preparation of MSN, was first optimized. With increasing concentration of AP from 0 to 40 mg mL^{-1}, the HPLC signal of the released AP increased and trended to plateau at 35 mg mL^{-1} (Fig. 3A). So, 35 mg mL^{-1} of AP was chosen for the preparation of MSN. To investigate the effect of the concentration of aptamer on the detection system, aptamer at different concentrations ranging from 0 to 60 μM was optimized. As shown in Fig. 3B, the signal intensity of the system decreased as the concentration of aptamer increased. Furthermore, the optimum concentration of aptamer used in this system was 40 μM. The reaction time was another important parameter affecting the analytical performance. It was clear that the signal response increased with the increase of reaction time and tended to a maximum value at 60 min (Fig. 3C). In order to minimize nonspecific leaking of the dye molecule from the particles, 60 min was chosen as the detection time point. Since the adsorption of aptamer on the MSN is based on the

electrostatic interaction, the pH of the reaction solution should be important for the analytical performance of the aptamer-ATP. In this case, aptamer-MSN was initially prepared in pH 7.4 HB system, and then the as-prepared MSN-aptamer was redispersed into various-pH HB solutions in the absence of target ATP. The resulting supernatant was monitored by the mentioned-above method. As indicated from Fig. 3D, the signal intensity almost tended to level off when pH of HB was higher than 6. In contrast, the signal intensity increased with the decreasing pH of PBS from 6 to 3.5. The reason might be most likely a consequence of the fact that partial aptamer-MSN conjugates were separated each other owing to the formation of MSN-APTES with negative charge or without charge when pH of HB was ≤6, thereby resulting in the release of the entrapped AP from the pores. Considering the bioactivity of the conjugated ATP and the capping efficiency of aptamer-MSN toward AP by APTES, however, pH 7.4 of HB was used as the reaction solution for detection of ATP.

3.5 Performance of the ATP aptasensor.

Under the optimal conditions, the developed method was employed for quantifying ATP standards with various concentrations based on target-responsive controlled release of AP from aptamer-gated MSN nanocontainers. As shown in Fig. 4, the HPLC signal increased with the concentration of ATP ranging from 1 nM to 10 μM. The maximum release was observed at 10 μM of ATP, suggesting that the ATP aptamer combined with ATP thoroughly at this ATP concentration. The corresponding calibration plots were demonstrated in the inset, it was found the increased HPLC peak area exhibited a good liner relationship with the concentration of ATP. The linear

equation was fitted as I = 13477 log *c* + 127025 (R = 0.9889). The limit of detection (LOD) was 0.41 nM at a signal-to-noise ratio of 3σ (where σ is the standard deviation of a blank solution). To confirm that the high sensitivity of the current strategy was the consequence of the target-induced structure switching of aptamers functionalization mesoporous silica nanoparticle, control experiments only at different target concentrations were direct conducted by HPLC. As shown in Fig. S2, the intensity decreased with the increasing concentration of target in the range from 100 nM to 1 mM. The detection limit was 31 nM. Additionally, detection performances of the proposed method were compared with that of other approaches for ATP detection and the results were shown in Table 1. Such comparison reflected that the proposed aptasensor exhibited much higher sensitivity, which provided a powerful evidence of our strategy for sensitive detection of ATP. The above results indicated the successful achievement of the HPLC amplified ATP detection, which should be attributed to the factor: The key advantage of this stimulus-release system is the signal amplification process. Because of the unique hollow structure and large inner space of MSN, a large number of dye molecules can be trapped, but only a small concentration of the "key" molecule (ATP in this paper) is required to uncap an MSN pore and release a large amount of dye molecules to generate a high HPLC signal. Thus the results identified that this signal amplification method was efficient for sensitive HPLC detection of ATP.

3.6 Specificity and practicability of the aptasensor.

In order to investigate the specific response of the biosensor to ATP, control

experiments were performed by incubating the biosensors in several aqueous solutions containing 0.1 μM ATP, UTP, CTP and GTP, respectively. A HB solution was used as blank. It was shown in Fig. 5 of the supplementary material that only ATP samples gave obvious HPLC intensity changes, while UTP, CTP and GTP samples delivered the same intensity as blank sample. This proves that the ATP-binding aptamer sequence is very specific to ATP. The cross-sensitivity of the sensor in a mixture with three different nucleosides containing ATP was also examined. The signal obtained from the complex was similar to that obtained from ATP only, which further indicated that the HPLC biosensor was very specific for ATP determination with negligible response to UTP, CTP and GTP. Furthermore, the approach has the limitation to distinguish ATP from its analogues like adenosine, AMP, and ADP (Fig. S3), because the ATP aptamer recognizes the adenine and ribose moieties, not the phosphate moiety. In order to solve this defect, further study is under investigation in our lab. The low CVs indicated the possibility of aptamer-MSN batch preparation. When the as-prepared aptamer-MSN was not in use, it was stored in pH 7.4 HB at 4 °C. No obvious change in the signal was observed after storage for 7 days but a 5% decrease of the current was noticed at 14 th day.

3.7 Analysis of ATP in human serum.

To further monitor the possible application of the developed aptasensor for the analysis of real samples, 4 ATP standards including 1.0 μM, 100 nM, 10 nM and 1.0 nM ATP were spiked into human serum samples, respectively. Then, these samples were measured by using the newly prepared aptasensor. The assay results were

calculated according to the mentioned-above linear regression equation. As shown in Table 2, the recoveries for the added ATP fall in the range from 97.6% to 105%, indicating that the proposed ATP sensing method can be applied for real samples. Therefore, the developed aptasensor could be utilized for the detection of target ATP in real samples.

4. Conclusion

In summary, we developed a simple and sensitive HPLC aptasensor for ATP detection based on target induced displacement reaction accompanying the release of cargo from aptamer-gated mesoporous silica nanocontainers. The results demonstrated that the system had a high loading amount of guests and good release behavior in the presence of ATP. The proposed assay shows a wide detection range, low limit of detection, and acceptable accuracy. Compared with conventional HPLC, the released dye molecules by the trigger of target can afford the strong HPLC intensity. Significantly, the assay can be easily extended for use with other food-relevant toxins by controlling the used target antibody, thus representing a versatile detection method.

Acknowledgment

This work was supported by the National Natural Science Foundation of China (21405130), and Excellent Talents of Xuzhou Medical College (D2014007), and State Key Laboratory of Analytical Chemical for Life Science (SKLACLS1405).

References

1. W. Yao, L. Wang, H. Y. Wang, X. L. Zhang and L. Li, *Biosens. Bioelectron.*, 2009, **24**, 3269–3274.

2. Y. Y. Xu, J. Xu, Y. Xiang, R. Yuan and Y. Q. Chai, *Biosens. Bioelectron.*, 2014, **51**, 293–296.

3. F. Li, Z. F. Du, L. M. Yang and B. Tang, *Biosens. Bioelectron*., 2013, **41**, 907–910

4. Y. H. Song, X. Yang, Z. Q. Li, Y. J. Zhao and A. P. Fan, *Biosens. Bioelectron*., 2014, **51**, 232–237.

5. Y. T. Liu, J. P. Lei, Y. Huang and H. X. Ju, *Anal. Chem*., 2014, **86**, 8735–8741.

6. S. F. Liu, Y. Wang, C. X. Zhang, Y. Lin and F. Li, *Chem. Commun*., 2013, **49**, 2335–2337

7. X. L. Zhu, B. Zhang, Z. H. Ye, H. Shi, Y. L. Shen and G. X. Li, *Chem. Commun*., 2015, **51**, 640–643.

8. X. R. Zhang, Y. Q. Zhao, S. G. Li and S. S. Zhang, *Chem. Commun.*, 2010, **46**, 9173–9175.

9. Z. Y. Lin, F. Luo, Q. D. Liu, L. F. Chen, B. Qiu, Z. W. Cai and G. N. Chen, *Chem. Commun.*, 2011, **47**, 8064–8066.

10. T. Bao, H. W. Shu, W. Wen, X. H. Zhang and S. F. Wang, *Anal. Chim. Acta*., 2015, **862**, 64–69.

11. M. Michaud, E. Jourdan, A. Villet, A. Ravel, C. Grosset and E. Peyrin, *J. Am. Chem. Soc*., 2003, **125**, 8672–8679.

12. X. F. Xue, F. Wang, J. H. Zhou, F. Chen, Y. Li and J. Zhao, *J. Agr. Food Chem*., 2009, **57**, 4500–4505.

13. G. V. Zyryanov, M. A. Palacios and P. Anzenbacher, *Angew. Chem. Int. Ed*., 2007, **46**, 7849–7852.

14. G. Carrea, R. Bovara, G. Mazzola, S. Girotti, A. Roda and S. Ghini, *Anal. Chem.*, 1986, **58**, 331–333.

15. D. Compagnone, G. G. Guilbault, *Anal. Chim. Acta.*, 1997, **340**, 109–113.

16. M. Michaud, E. Jourdan, A. Villet, A. Ravel and C. E. GrossetPeyrin, *J. Am. Chem. Soc.*, 2003, **125**, 8672–8679

17. X. F. Xue, F. Wang, J. H. Zhou, F. Chen, Y. Li and J. Zhao, *J. Agr. Food Chem.*, 2009, **57**, 4500–4505.

18. J. Zhang, P. P. Chen, X. Y. Wu, J. H. Chen, L. J. Xu, G. N. Chen and F. F. Fu, *Biosens. Bioelectron.*, 2011, **26**, 2645–2650.

19. Z. B. Chen, Y. Tan, C. M. Zhang, L. Yin, H. Ma, N. S. Ye, H. Qiang and Y. Q. Lin, *Biosens. Bioelectron.*, 2014, **56**, 46–50.

20. Y. Li, H. L. Qi, Y. G. Peng, Q. Gao and C. X. Zhang, *Electrochem. Comm.*, 2008, 10, 1322–1325.

21. X. Y. Wang, P. Dong, W. Yun, Y. Xu, P. G. He and Y. Z. Fang, *Biosens. Bioelectron.*, 2009, **24**, 3288–3292.

22. K. J. Feng, R. M. Kong, H. Wang, S. F. Zhang and F. L. Qu, *Biosens. Bioelectron.*, 2012, **38**, 121–125.

23. D. Wu, X. Ren, L. H. Hu, D. W. Fan, Y. Zheng and Q. Wei, *Biosens. Bioelectron.*, 2015, **74**, 391–397.

24. L. Wu, X. H. Zhang, W. Liu, E. H. Xiong and J. H. Chen, *Anal. Chem.*, 2013, **85**, 8397–8402.

25. H. Kuang, H. H. Yin, L. Q. Liu, L. G. Xu, W. Ma and C. L. Xu, *ACS Appl. Mater.*

Interfaces., 2014, **6**, 364–369.

26. S. Y. Li, D. Y. Chen, Q. T. Zhou, W. Wang, L. F. Gao, J. Jiang, H. J. Liang, Y. Z. Liu, G. L. Liang and H. Cui, *Anal. Chem*., 2014. **86**, 5559–5566.
27. C. L. Zhu, C. H. Lu, X. Y. Song, H. H. Yang and X. R. Wang, *J. Am. Chem. Soc*., 2011, **133**, 1278-1281.
28. X. X. He, Y. X. Zhao, D. G. He, K. Wang, F. Z. Xu and J. L. Tang, *Langmuir*., 2012, **28**, 12909-12915.
29. K. Y. Wang, J. Liao, X. Y. Yang, M. Zhao, M. Chen, W. R. Yao, W. H. Tan and X. P. Lan, *Biosens. Bioelectron*., 2015, **63**, 172–177.
30. J. F. Xia, D. M. Song, Z. H. Wang, F. F. Zhang, M. Yang, R. J. Gui, L. Xia, S. Bi, Y. Z. Xia, Y. H .Li and L. H. Xia, *Biosens. Bioelectron*., 2015, **68**, 55–61.
31. R. Casasus, E. Climent, M. D. Marcos, R. Martínez-Manez, F. Sancenon, J. Soto, P. Amoros, J. Cano and E. Ruiz, *J. Am. Chem. Soc*., 2008, **130**, 1903−1917.
32. E. Aznar, M. D. Marcos, R. Martínez-Manez, F. Sancenon, J. Soto, P. Amoros and C. Guillem, *J. Am. Chem. Soc*., 2009, **131**, 6833−6843
33. J. L. Vivero-Escoto, I. I. Slowing, B. G. Trewyn and V. S. Y. Lin, *Small*., 2010, **6**, 1952−1967.
34. E. Climent, R. Martinez-Manez, F. Sancenon, M. D. Marcos, J. Soto, A. Maquieira and P. Amoros, *Angew. Chem. Int. Ed*., 2010, **49,** 7281−7283
35. Y. F. Zhang, Q. Yuan, T. Chen, X. B. Zhang, Y. Chen and W. H. Tan, *Anal. Chem*., 2012, **84**, 1956-1962.
36. X. M. Wang, M. R. Cui, H. Zhou and S. S. Zhang, *Chem. Comm*., 2015, **51**,13983-13985.

37. R. Liu, X. Zhao, T. Wu and P. Feng, *J. Am. Chem. Soc*., 2008, **130**, 14418−14419.

38. C. Park, H. Kim, S. Kim and C. Kim, *J. Am. Chem. Soc*., 2009, **131,** 16614−16615.

39. J. L. Vivero-Escoto, I. I. Slowing, C. W. Wu and V. S. Y. Lin, *J. Am. Chem. Soc*., 2009, 131, 3462−3463.

40. C. Park, K. Lee and C. Kim, *Angew. Chem., Int. Ed.*, 2009, **48,** 1275−1278.

41. A. Schlossbauer, S. Warncke, P. M. E. Gramlich, J. Kecht, A. Manetto, T. Carell and T. Bein, *Angew. Chem. Int. Ed*., 2010, **49**, 4734−4737.

42. B. Zhang, B. Q. Liu, J. Y. Liao, G. N. Chen and D. P. Tang, *Anal. Chem*., 2013, **85**, 9245−9252.

43. Z. X. Zhang, D. Balogh, F. Wang, S. Y. Sung, R. Nechushtai and I. Willner, *ACS Nano*, 2013, **7**, 8455-8468.

44. E. Climent, R. Martinez-Manez, F. Sancenon, M. D. Marcos, J. Soto, A. Maquieira and P. Amoros, *Angew. Chem., Int. Ed.*, 2010, **49**, 7281−7283.

45. K. L. Kashefi and M. A. Mehrgardi, *Biosens. Bioelectron.*, 2012, **37**, 94–98.

46. X. L. Zuo, S. P. Song, J. Zhang, D. Pan, L. H. Wang, C. H. Fan, *J. Am. Chem. Soc*., 2007, **129**, 1042–1043.

47. K. W. Ren, J. Wu, Y. Zhang, F. Yan, and H. X. Ju, *Anal. Chem.*, 2014, **86**, 7494−7499.

Figure captions

Scheme 1 Schematic Illustration of high-performance liquid chromatography detection of ATP based on target-induced structure switching of aptamers functionalization mesoporous silica nanoparticle.

Fig. 1 (A) TEM image, (B) DLS characterization, and (C) nitrogen adsorption−desorption isotherm of MSNs. Inset in C: pore size distribution. (D) Zeta-potential analysis of MS nanoparticles (a), amine-functionalized MS nanoparticles (b), MB-MS nanoparticles (c), and MSN (d).

Fig. 2 HPLC of (a) blank (HB); (b) MSN; (c) ATP and MSN for 10 min; (d) ATP and MSN for 60 min.

Fig. 3 Dependence of HPLC signals intensity on (A) AP concentration for preparation of MSN, (B) the concentration of aptamer, (C) reaction time in the absence of target (a) or in the presence of target (b); and (D) pH. When one parameter changes the others are under their optimal conditions.

Fig. 4 (A) HPLC responses of ATP at concentrations of 1.0 nM to 10 μM (from a to e), and (B) calibration curve. Error bars represent standard deviations of three parallel experiments.

Fig. 5 Histograms of the selectivity of the aptamer−MSN system examined by being incubated in the following samples under the same experimental conditions: (a) blank; (b) GTP, (c) CTP, (d) UTP, (e) ATP, and (f) GTP + CTP + UTP + ATP; the concentration of ATP, CTP, UTP, and GTP is 0.1μM, respectively.

Table 1. Comparing of the proposed method with the ATP assays using aptamer as a recognition molecule.

Analytical method	Detection limit	Linear range	Refs.
Fluorescence	1 mM	1 mM to 8 mM	Ref. 27
Fluorescence	1 mM	1 mM to 20 mM	Ref. 28
Fluorescence	5.2 nM	10 nM to 100 μM	Ref. 29
Electrochemical	1 μM	1 μM to 3 mM	Ref. 45
Electrochemical	10 nM	10 nM to 1 mM	Ref. 46
HPLC	0.41 nM	1 nM to 10 μM	This work

Table 2 Analysis of ATP in human serum samples.

Sample	Added ATP	Our proposed method	RSD (%)	Recovery (%)
1	1 μM	1.02 μM	3.3	102
2	100 nM	97.6 nM	4.1	97.6
3	10 nM	10.4 nM	2.8	104
4	1.0 nM	1.05 nM	3.2	105

Scheme 1

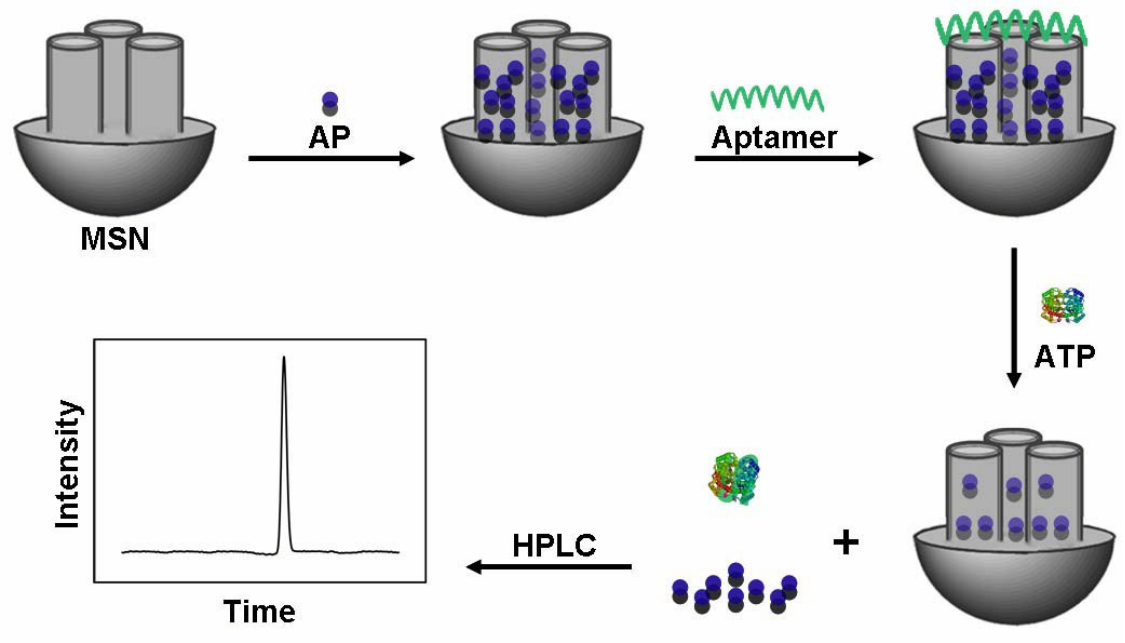

Fig.1

Fig.2

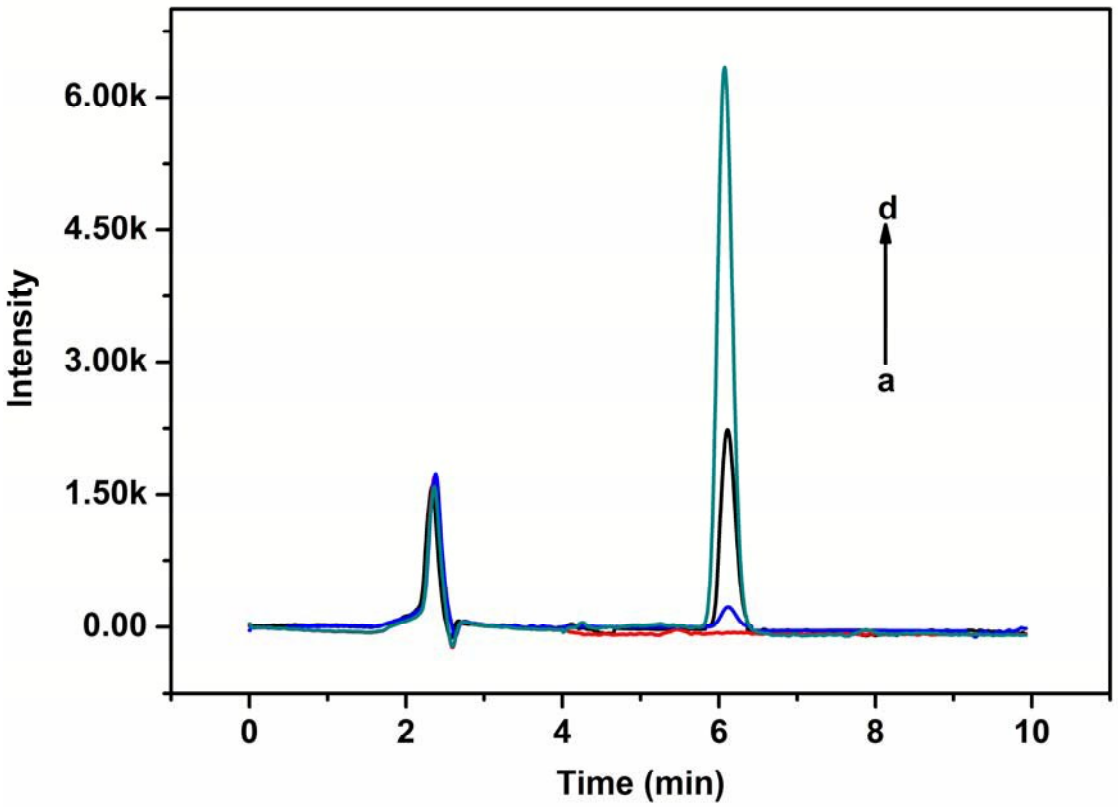

Fig.3

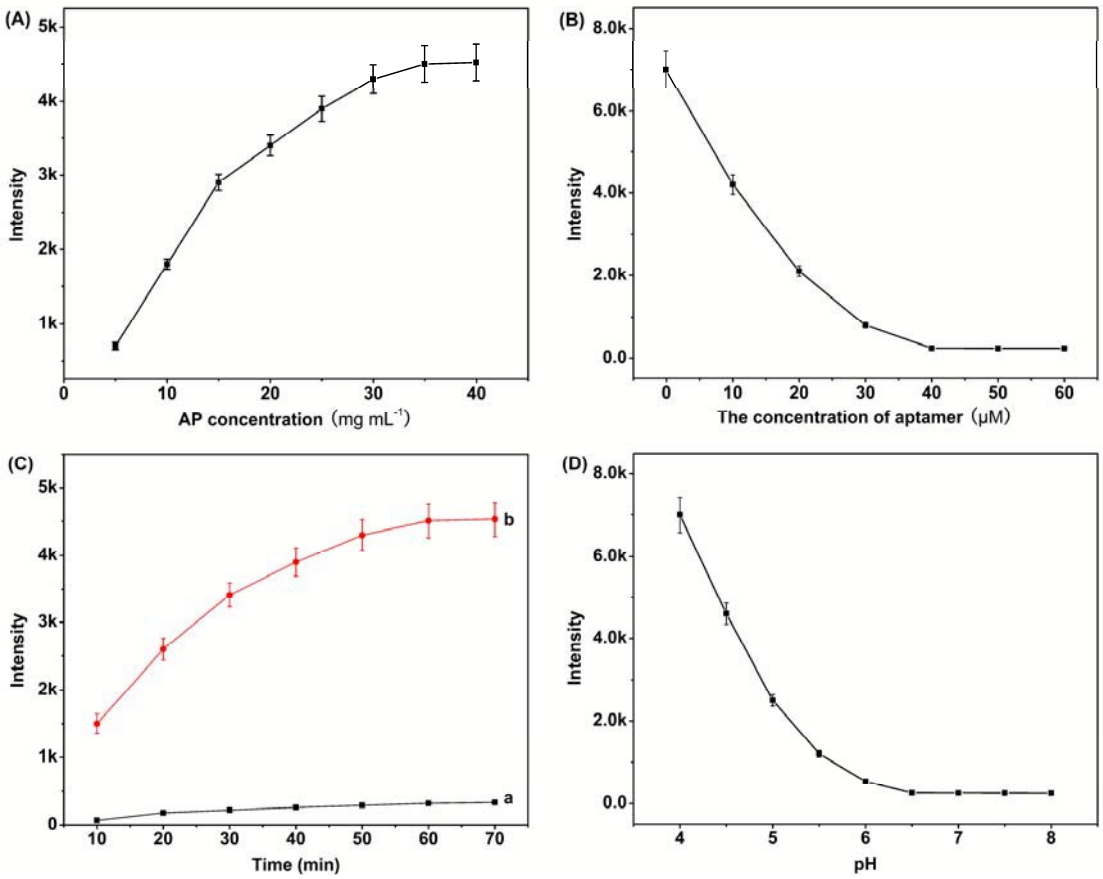

Fig.4

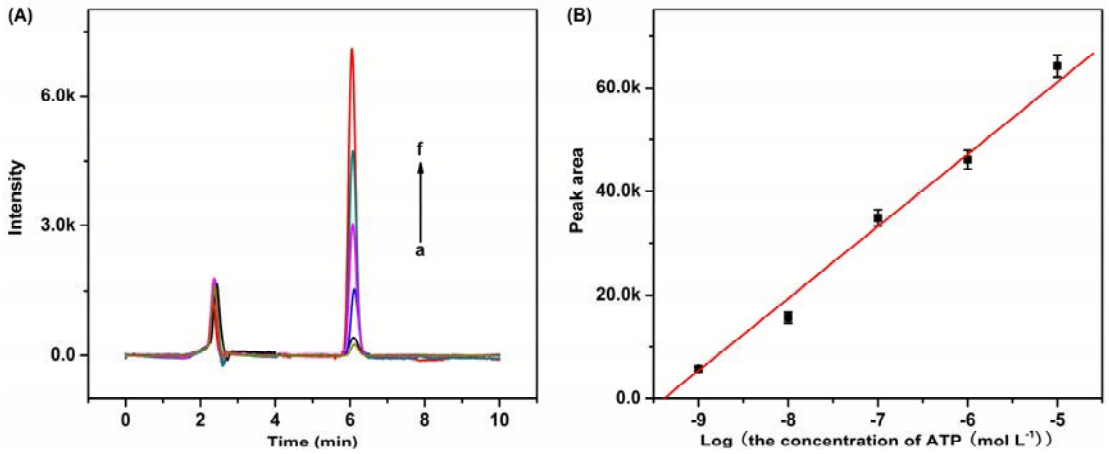

Fig.5

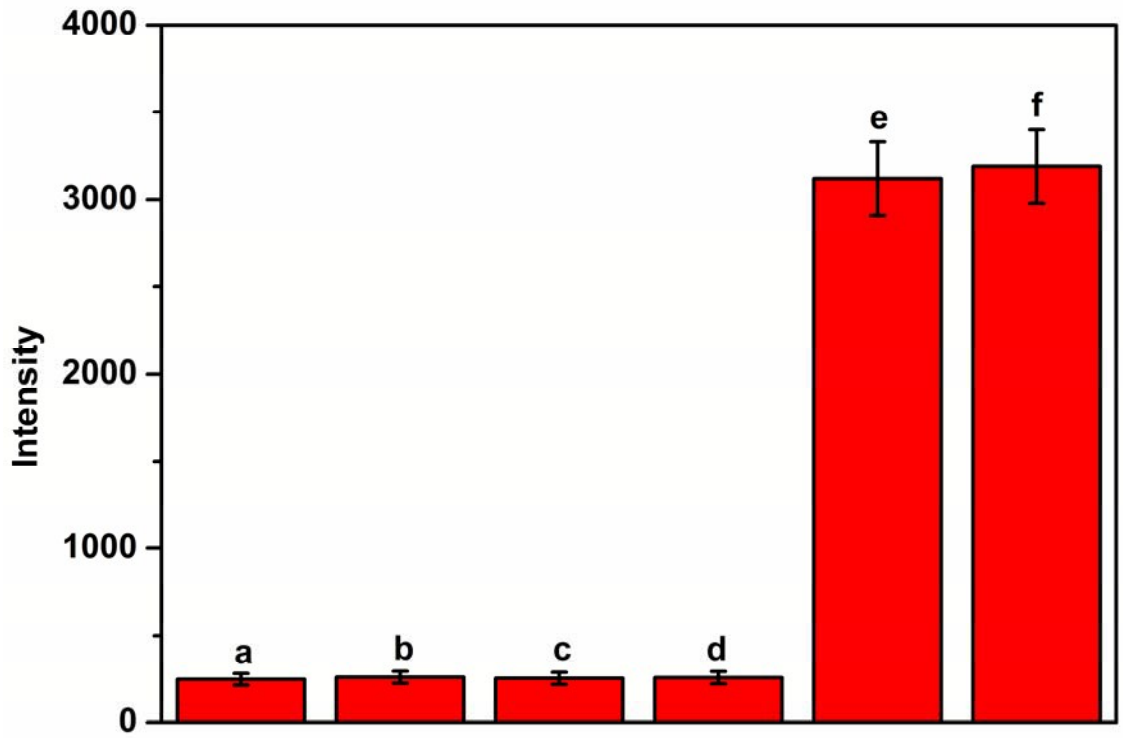

Graphical Abstract:

By Lili Du, Yu Zhang, Yan Du, Dongzhi Yang, Fenglei Gao*, and Daoquan Tang*

Jiangsu Key Laboratory of New Drug Research and Clinical Pharmacy, School of Pharmacy, Xuzhou Medical College, 221004, Xuzhou, China.

A strategy for high-performance liquid chromatography detection of adenosine triphosphate was developed based on mesoporous silica nanoparticles functionalized with an aptamer as cap.